Applications of Nuclear Techniques (CRETE13)
International Journal of Modern Physics: Conference Series
Vol. 27 (2014) 1460136 (7 pages)

DOI: 10.1142/S2010194514601367

World Scientific
www.worldscientific.com

ACHIEVING A LINEAR DOSE RATE RESPONSE IN PULSE-MODE SILICON PHOTODIODE SCINTILLATION DETECTORS OVER A WIDE RANGE OF EXCITATIONS

LEWIS CARROLL

Carroll & Ramsey Associates, 950 Gilman St., Suite 105
Berkeley, CA 94705 USA
cra@carroll-ramsey.com

Published 25 February 2014

We are developing a new dose calibrator for nuclear pharmacies that can measure radioactivity in a vial or syringe without handling it directly or removing it from its transport shield "pig". The calibrator's detector comprises twin opposing scintillating crystals coupled to Si photodiodes and current-amplifying trans-resistance amplifiers. Such a scheme is inherently linear with respect to dose rate over a wide range of radiation intensities, but accuracy at low activity levels may be impaired, beyond the effects of meager photon statistics, by baseline fluctuation and drift inevitably present in high-gain, current-mode photodiode amplifiers. The work described here is motivated by our desire to enhance accuracy at low excitations while maintaining linearity at high excitations. Thus, we are also evaluating a novel "pulse-mode" analog signal processing scheme that employs a linear threshold discriminator to virtually eliminate baseline fluctuation and drift. We will show the results of a side-by-side comparison of current-mode versus pulse-mode signal processing schemes, including perturbing factors affecting linearity and accuracy at very low and very high excitations. Bench testing over a wide range of excitations is done using a Poisson random pulse generator plus an LED light source to simulate excitations up to ~10^6 detected counts per second without the need to handle and store large amounts of radioactive material.

Keywords: Scintillation detectors; dynamic range; baseline stabilizer.

1. Introduction

A scintillation detector operating in "pulse mode", with a threshold discriminator to eliminate baseline fluctuation and drift, is ideal for measuring low to moderate levels of activity. Figure 1 illustrates a simple bench experiment, where a small (~35 nCi) ^{22}Na check source is quickly placed next to one of our 10 cm^3 pulse-mode CsI(Tl) scintillation probes, then quickly removed, then repeated. We performed the same moves with a similar probe operating in DC current mode.

The radiation-induced photo-current in both cases is of the order of 600 fA; the integrating filter time constant is of the order of ~2 s. The zero-peak detector output

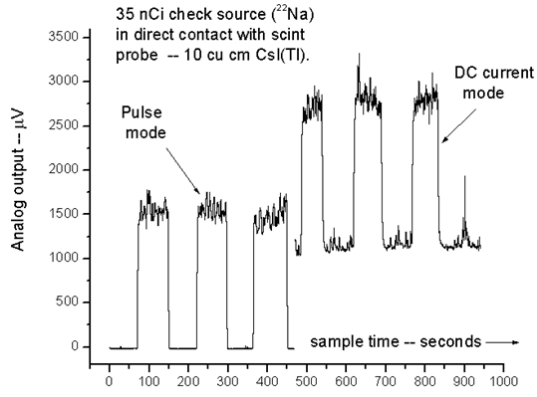

Fig. 1. Step response at low excitation.

signal amplitude in each case is small, only ~1.5 mV, but since noise and fluctuations are eliminated by the action of the threshold discriminator in the pulse-mode detector, its baseline is flat and virtually noise free, enhancing signal detectability in that system.

However, a scintillation detector operating in non-counting DC current mode should be capable of linear response over a much wider range of activities since there is no counting loss due to saturation effects or detector system dead time.

Is there a way to exploit the superior signal detectability of pulse-mode detection at low excitations, while maintaining the superior linearity of DC current mode detection at high excitations? Perhaps, provided we are willing to abandon the notion of pulse-counting, *per se*, and concentrate instead on carefully preserving the mean value of the raw analog signal pulses. We have indeed found a way to extend the useful range of our pulse-mode scintillation detectors to allow operation at substantially higher radiation exposure levels while maintaining the inherent sensitivity and clean baseline characteristic at low exposure levels.

2. Stress-Testing at High Count Rates

To facilitate our development effort, we employed a quad array of home-made random pulse generators,[1] each generator driving separate light-emitting diodes (LEDs) which together illuminate a single Si PIN photodiode plus charge-integrating preamplifier to emulate our scintillation probe's front end.[2] This apparatus allowed us to perform multiple, rapid, and repeated trials at various levels of excitation without having to handle large amounts of radioactive material. The "Poisson-ness" of our random pulse generators was validated against a calibrated time-to-amplitude converter in conjunction with a multichannel analyzer.

3. Salient Details

Key elements of our new pulse-mode detector scheme are shown in Fig. 2.[3] The scintillation probe's preamplifier, which is pole-zero compensated to minimize pulse

undershoot,[4] is connected to a post-amplifier comprising two parts: a high-gain, wide-band first amplifying circuit, followed by a low gain (~2) constrained bandwidth (low-pass) shaping amplifier circuit.

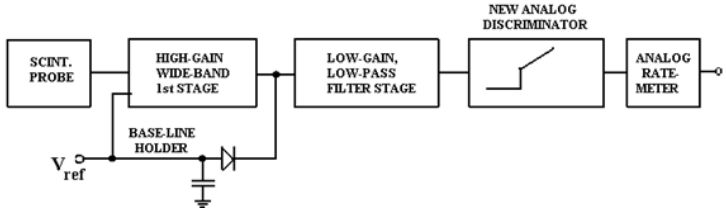

Fig. 2. System block diagram.

The wide band first stage incorporates a negative-rectifying-diode, baseline holder feedback loop,[5] which serves to establish a defined baseline reference, or common-potential terminal V_{ref} for use in subsequent amplifier stages and circuit functions. Note that the baseline holder function is typically applied to the output of the low-pass shaping amplifier in order to stabilize the baseline for use in spectroscopy. Here, however, our aim is quite different, as we intend to push the system to extreme count rates. Thus, we derive our baseline reference instead from the wide bandwidth first amplifying circuit.

The amplifier stages are all DC-coupled in order to preserve the mean value of the analog waveform relative to V_{ref}. At extremely high count rates, the signal waveform no longer consists of discrete, recognizable pulses, but rather resembles a noisy continuum. The low-pass filter stage tends to attenuate or "shrink" this waveform toward the mean. As the pulse rate increases, the low-pass filtered waveform cannot return to the actual reference potential and therefore appears to "levitate" relative to V_{ref}, as shown in the oscilloscope traces in Fig. 3.

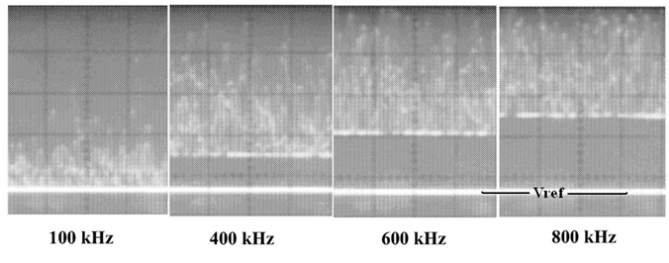

Fig. 3. "Levitating" analog waveform.

4. Analog Discriminator

The shaping amplifier is followed by an analog threshold discriminator whose input-output characteristic is denoted by the sketch in the block labeled "new analog discriminator" shown in Fig. 2. This circuit combines the dual functions of a threshold

discriminator and a linear gate in which the gate pedestal is set equal to the threshold setting.[6] Pulse signals (or noise) whose peak amplitude is less than the threshold setting are blocked and are not transmitted through to the output. Pulse signals whose amplitude exceeds the threshold are transmitted through and are fully and linearly reproduced at the output.

Further, as the radiation field intensity and consequent signal pulse rate increases to the point where pulses overlap many times over, noise is no longer an issue. The analog waveform can "levitate" to a level that exceeds the threshold setting and is therefore transmitted directly through the analog discriminator to the rate-meter circuit — a low-pass filter with a slow (1–2 s) time constant and which, in turn, displays the running mean value of dose rate in the detector probe.

5. Operation at very High Exposure Dose Rates

The usual counting type pulse-mode detector system suffers from saturation effects due to detector system dead time at high dose rates. The governing parameter is the signal pulse width; narrow is better than wide, except for the effects of noise, which is inherent and ever-present in a solid-state detector operating at room temperature. In our case, the low-pass-filtered pulse width is on the order of 25 μs in order to optimize signal-to-noise ratio at low pulse rates.

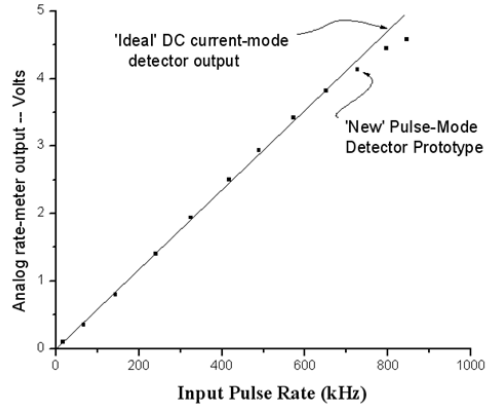

Fig. 4. Prototype detector output at high dose rate.

Based on standard textbook models of dead time,[7] a counting-type pulse-mode detector with 25 μs wide pulses should begin to show signs of saturation at count rates as low as a few 10s of kHz. However, with our new analog signal processing scheme, the conventional textbook dead time models no longer apply, and we are able to demonstrate a linear dose rate response for detected pulse rates up to ~800 kHz before saturation effects begin to set in as can be seen in Fig. 4.

6. Operation at very Low Exposure Dose Rates

Assuming that the analog threshold discriminator is properly set to eliminate the effects of electronic noise and drift with time and temperature, the ability to detect and measure very low levels of radiation exposure dose rate is governed primarily by fluctuation in the output time record due to statistical fluctuation of the ambient radiation background.

There is a rich literature on the subject of detector system design for extreme low-level counting in fields such as radiocarbon dating, but in this work, we stipulate only that, in order to minimize exposure to the ambient photon radiation present in the lab, the scintillation probe is embedded in a shield comprising a lead cube, ~15 cm on a side.

During development of our wide dynamic range pulse-mode detector, we observed occasional spurious "glitches" or spikes in the time record of the detector's rate meter output when no radiation source was present (see Fig. 5). These spikes were rarely observed in our smallest 1 cm^3 probes but were clearly present in 10 cm^3 and larger probes. The output spikes varied in amplitude every few hours and at any time of the night or day, some peaking as high as several tens of mV and occurring at random times.

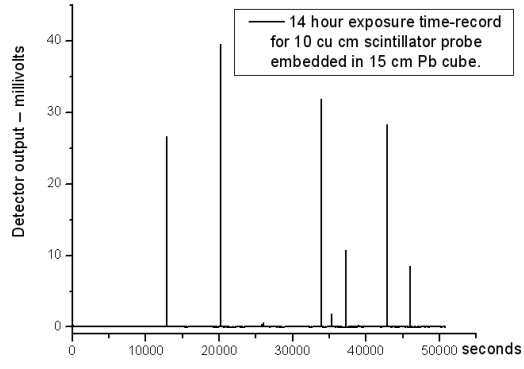

Fig. 5. Unwanted "glitches" in the time record.

Such random spikes in the time record could potentially cause errors and ambiguity by creating false peaks in applications such as chromatography. We found that a few of the spikes in the detector's rate meter output time record were caused by transient electromagnetic interference (EMI) from on-off electrical switch action from equipment plugged into nearby power outlets. One of the worst offenders was a temperature-controlled soldering iron that was inadvertently left plugged in and running on our lab bench. The on-off thermostatic control does not produce a clean electrical contact action but generates a burst of short but intense pulses — a burst sometimes lasting as long as several milliseconds. Fortunately, this problem was easily overcome by installing an EMI-reducing power mains filter on the input to the detector's power supply.

By far, however, most of the unwanted stray glitches in the time record were induced by singular, extreme-energy events that generated signal pulses of such a high amplitude as to hit the +24 VDC power supply rail, saturating the post-amplifier and causing a

corresponding transient disturbance in the baseline holder control circuitry that further exacerbated the effect.

7. Cosmic Rays

A search of the literature convinced us that this problem was caused by cosmic-ray-induced secondary muons and related electromagnetic cascades.[8] To further characterize this phenomenon, we conducted long-duration, high-energy background spectrum-recording experiments with Pb-shielded CsI(Tl) crystals of different sizes, as shown in Fig. 6. For this test only, our normal post-amplifier system gain was reduced by a factor of 10 in order to accept and record the highest energies. Note that some extreme outlier events were recorded with energies greater than 100 MeV!

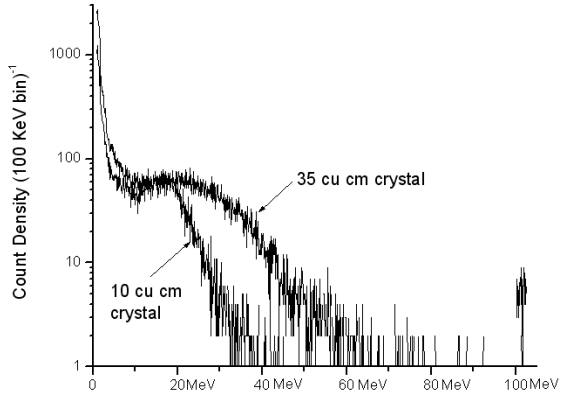

Fig. 6. 24 hour background spectrum.

8. Amplitude Limiting

In order to achieve our original goal of realizing a linear detector response at very high exposure dose rates, we had initially refrained from incorporating any sort of upper level threshold discriminator or similar amplitude-limiting circuitry. However, in light of this cosmic-ray-induced transient-impulse phenomenon, we reasoned that a dynamic signal-clamping threshold scheme could mitigate the problem at very low levels of exposure by limiting the peak signal pulse amplitude to a credible "earthly" maximum of ~2.5 MeV for a single pulse, but which would gradually rise so as to eliminate the clamping effect at higher exposure levels when the consequence of any such signal spikes becomes small relative to the total exposure dose rate.

The dynamic signal-clamping scheme, plus some further circuit changes (revised baseline holder feedback control parameters, loop gain, integrating filter time constants, *etc.*,) consistent with the circuit topology shown in Fig. 2, finally put this problem to rest.

Figure 7 shows an overnight ambient exposure dose rate time record comparing our new analog pulse-mode prototype with a DC current-mode type of detector with the same

overall gain and filter time constant. Note that the baseline is much cleaner on the pulse-mode detector and that, while transient glitches are still visible in both DC current and pulse-mode detectors, the latter are now much lower in amplitude.

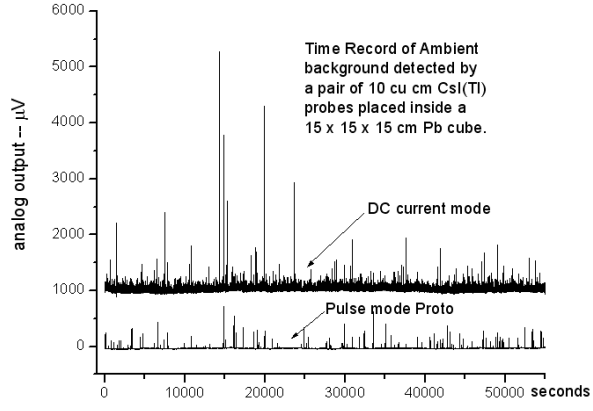

Fig. 7. Overnight time record.

9. Conclusion

We have demonstrated an analog non-counting type of solid-state Si PIN diode-based pulse-mode scintillation detector scheme that provides a clean, drift-free and relatively glitch-free baseline at low radiation exposures, while achieving linear response comparable to that of a DC current mode type of detector at count rates up to several 100s of kHz.

References

1. G. H. White, *J. Sci. Instrum.* **41**(6), 361 (1964).
2. Lewis R. Carroll, Charge-Integrating Preamplifier for Capacitive Transducer, US Patent Number 6,054,705 (April, 2000), http://www.patentbuddy.com/Patent/6054705.
3. Lewis R. Carroll, Method and Apparatus for Extending a Scintillation Counter's Dynamic Range, US Patent application #13/048,266, http://www.google.com/patents/US20110284753.
4. W. R. Leo, in *Techniques for Nuclear and Particle Physics Experiments: A How-To Approach* (Springer Verlag, New York, 1994), ch. 14, ISBN 0-387-57280.
5. L. V. East, *Rev. Sci. Instrum.* **41**, 1245 (1970).
6. W. R. Leo, *op. cit.*
7. Glen F. Knoll, in *Radiation Detection and Measurement* (John Wiley and Sons, New York, 1979), ch. 3.
8. P. Theodorsson, in *Measurement of Weak Radioactivity* (World Scientific Publishing Company, Singapore, 1996), Fig. 11.3.